Enhancement of photocatalytic property on ZnS/MoS2 composite under visible light irradiation

Jiushan Cheng[1,2], Lu Han[1], Yen Wei[2] and Qiang Chen[1]

[1]*Laboratory of Plasma Physics and Materials, Beijing Institute of Graphic Communication, Beijing 102600, China*
[2]*Department of Chemistry and the Tisnghua Center for Frontier Polymer Research, Tsinghua University, Beijing, 10084, China*

Abstract: In this paper, the composite ZnS/MoS_2 was obtained via two steps including solvothermal methods. The as-synthesized sample was characterized by X-ray diffraction (XRD), scanning electron microscopy (SEM) and UV-Vis. diffuse reflectance spectra (DRS). The photocatalytic activity of the product was evaluated through photocatalytic degradation of Rhodamine B (Rh B) under UV-Vis. light irradiation; the electrical conductivity of ZnS/MoS_2 composites was significantly improved compared to ZnS, MoS_2, respectively. The results showed that the ZnS/MoS_2 composite photocatalyst possesses better photocatalytic activity in degrading Rh B than the single ZnS or the single MoS_2. The better photocatalytic properties may be due to the synergetic effect of two semiconductors, because of which electrons and holes were separated effectively. And its specific microstructure played an active role in evaluating photocatalytic performance.

1 Introduction

Environmental degradation is one of the challenging phenomenons due to the increasing rate of the industrialization in the world wide. Especially, organic dyes have been wildly used in the plastic, paper, textile, and other chemical industries in our lives [1-3]. And it can cause environmental pollution.

However, photocatalysis is one of the promising methods to remove the organic components from waste water. Semiconductor photocatlysts have attracted a subject of extensive interest due to their fundamental importance applications for solving energy and pollution problems. Recently, molybdenum disulfide (MoS_2), shows great potential for visible light irradiated photocatalysis applications. More and more researchers have been extensively investigated MoS_2 as a promising candidate for many materials, due to its excellent electrical carrier mobility, high chemical reactivity and optical properties [4-7]. For instance, Xiuquan Gu [8] et al. obtained MoS_2/Ag_3PO_4 hybrids by incorporating MoS_2 nanosheets during the preparation process of Ag_3PO_4 microparticles. The paper pointed out that the photocatalytic activity of MoS_2/Ag_3PO_4 hybrid got improved owning to compositing with trace amounts MoS_2. The group of Aiyong Zhang [9] prepared layer-controlled MoS_2 on three-dimensional Bi_2S_3 micro-flower through sacrificial templating strategy. The paper showed that 3D flower-like hybrid nanostructures make MoS_2/ Bi_2S_3 to display great photocatalysis under visible light irradiation.

Similarly, among the plenty of metal sulfide photocatalysts, especially, ZnS, have been paid more attention from the scientific research owing to their optical properties and unique catalytic functions. However, ZnS is responsive only in ultraviolet light region. To address this issue, many means have been used, such as nanomaterials morphology modification and semiconductor compositing. These methods are proved to be effective, and the best way is meeting the energy demands of ZnS with wide band-gap to maintain the catalytic activity [10-11]. Longxin Hu [12] et al. reported that SnO_2/ZnS nanocomposite was prepared by one step hydrothermal method. It was found that the compound showed the great photocatalytic activity. The photocatalytic degradation of RhB (Rhoadmine B) reached 95% at given time. In Baibiao Huang's group [13], they prepared ZnS microspheres with Mn-doping by a facile solvothermal route. And it was found that Mn-doping ZnS exhibited better photocatalytic performance than pure ZnS.

Owing to there have been few studies related to ZnS/MoS_2 composite. In this paper, we successfully prepared semiconductor of MoS_2 decroated with ZnS as catalyst for efficient degradation of dye. Therefore, we pay attention to the ZnS nanoparticles coated MoS_2 nanosheets system connecting two chemically stable and inexpensive multifunctional semiconductor materials together. In this system, MoS_2 nanosheets work as narrow band gap p-type semiconductor and ZnS serves as wide band-gap n-type semiconductor. The experimental reagents are simple and easy to get and the reaction conditions are simple and controllable. Experiment results indicate that ZnS composite MoS_2 exhibit superior photocatalyst performance towards RhB.

2 Experimental

In a typical procedure, 1.5 mmol Na_2MoO_4 and 15 mmol $C_3H_7NO_2S$ were dissolved in 80 ml deionized water. Then, the solution was transferred into a Teflon-lined stainless-steel autoclave, which was sealed and heated at 220℃ for 24 h, and then cool down to room temperature. The as-prepared precipitates were washed by ethyl alcohol and distilled water three times respectively. Then the black powder was collected and dried in vacuum at 80℃ for 12 h. The black precipate was denoted as MoS_2. 0.1g thioacetamide(CH_3CSNH_2), 0.6758g zinc acetate ($Zn(CH_3COO)_2$) and 0.245g Sodium Sulfide (Na_2S) were dissolved in 20 ml deionized water. The mixture was full stirred for 2 h at room temperature. Then, the solution was transferred into a Teflon-lined stainless-steel autoclave, which was sealed and heated at 170℃ for 24 h, and then cool down to room temperature. Then, the precipitates were collected and washed by ethyl alcohol and distilled water three times respectively. Then obtained powder was dried in vacuum at 60℃ for 12 h. The final powder was called ZnS.

0.1 as-prepared MoS_2, and 0.2g Sodium dodecyl sulfate(SDS), 1.3516g zinc acetate, 0.49g Sodium Sulfide were dissolved in 60 ml deionized water. Then, the solution was transferred into a Teflon-lined stainless-steel autoclave, which was sealed and heated at 170℃ for 2 h, and then cool down to room temperature. Then, the precipitates were collected and washed by ethyl alcohol and distilled water three times respectively. Then obtained powder was dried in vacuum at 60℃ for 12 h which denoted as ZnS/MoS_2.

The as-prepared products were characterized by powder X-ray diffraction (XRD) in Bruker D8 diffractometer using Cu Kα radiation. The surface morphology of the samples were observed by a HITACHI S3500 scanning electron microscopy (SEM). The light absorption properties were measured using UV–Vis. diffuse reflectance spectrophotometer U-4100 (DRS) with a wavelength range of 300~800 nm.

The photocatalytic activity of the samples was determined by degradation of Rhoadmine B (RhB) in an aqueous solution under visible light irradiation. The photo degradation experiments were carried out under UV-Vis. light irradiation whose source was a 300W Xe lamp. The distance between the xenon lamp and the sample was about 50 cm. In the each experiment, 20 mg photocatalyst was added into 20 mL RhB solution (C_0=10 mg/L). Prior to irradiation, the suspension was sonicated for a few minutes and then magnetically stirred in dark for hours to obtain desorption– adsorption equilibrium. At given time intervals, 5 mL of the sample solution was collected and separated through centrifugation. The HITACHI U-4100 UV–Vis. spectrometer was used to determine the concentration of RhB solution during the photocatalytic degradation process.

The electrochemical properties of all the samples were studied using electrochemical workstation (PGZ402, VoltaLab, France) with a three-electrodecon figuration. The samples were then used to modify screen-printed carbon electrodes (SPCEs) to immobilize antibodies and enhance the electrochemical signals.1 μl of 1mg/ml ZnS、MoS_2 and ZnS/MoS_2 were spread on the working area of SPECs using a micropipette and the film was dried at room temperature, resepectively. All the cyclic voltammetry (CV) measurements were recorded in 0.1M phosphate buffer (PBS, pH7.4) containing 5mM $K_3[Fe(CN)_6]$ and $K_4[Fe(CN)_6]$ in the potential range of -1000 to +1000mV. A reproducible voltammogram was obtained under steady-state conditions after about five cycles. All the electrochemical impedance spectroscopy (EIS) measurements were carried out in 0.01M PBS containing 5mM $K_3[Fe(CN)_6]$ and $K_4[Fe(CN)_6]$ in a frequency range from 0.1 to 104 Hz at 220mV.

3 Results and discussion

The XRD patterns of the samples are presented in Figure. 1. There are no other phases and peaks of impurities, demonstrating that all the samples are pure. MoS_2 and ZnS possess the phases corresponding to JCPDS No. 37-1492(a = 3.161 Å and b = 3.161 Å, c = 12.299 Å) and 65-5476 (a=5.404Å, b=5.404 Å, and c=5.404 Å) respectively. The XRD pattern of the ZnS/MoS_2 nanohybrid shows MoS_2 major peaks at corresponding to （100），（103），（110） and there are peaks, like (111)、（220）、（311） observed related to ZnS. And, no other phase is detected in the ZnS/MoS_2 composite before and after the photocatalytic degradation, suggesting that the composite is stable and there is no chemical reaction between MoS_2 and ZnS.

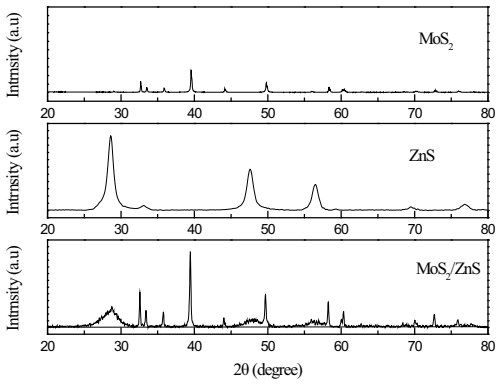

Figure 1. XRD pattern of the samples MoS_2, ZnS, ZnS/MoS_2.

The morphologies of the pure MoS_2, ZnS and ZnS/MoS_2 composite are observed by SEM. Figure.2a exhibits a representative SEM image of pure MoS_2. The highly monodispersed rough ball-like spheres are obtained which is composed of thin plates as shown in Figure.2b. The nanoplates align radically and tightly to assemble into the uniform spheres. The surfaces of nanoplates are smooth. The SEM micrograph of ZnS in Figure2c show a large number of plates arranged irregularly together. It can be seen the shapes of plate is the block shaped and the length is about 1 μm on average. Regarding to ZnS/MoS_2 composite, it could be seen that the microspheres are organized by hundreds of thin nanoplates and some ZnS plates are together with

sphere with a diameter of 1μm (Figure.2d).

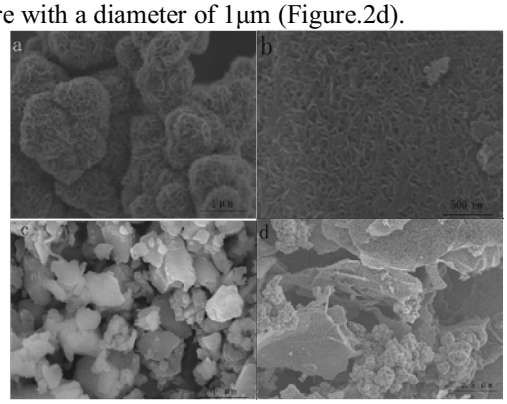

Figure 2. The SEM images of samples（a,b）MoS_2, (c) ZnS, (d) ZnS/MoS_2.

The absorption property is one of the most important properties to characterize the optical property of semiconductor. Figure.3 shows the UV-Vis. diffuse reflectance spectra of ZnS and ZnS/MoS_2 composite. It could be seen that the pure ZnS has an absorption edge occurred at about 375 nm. The absorption edge of the pure ZnS/MoS_2 is approximately at 390 nm. From the picture inset Figure.3, it can be seen UV-Vis. diffuse reflectance spectra of MoS_2. The absorption of ZnS/MoS_2 composite during visible light range is much improved may be owing to MoS_2 which plays an important role.

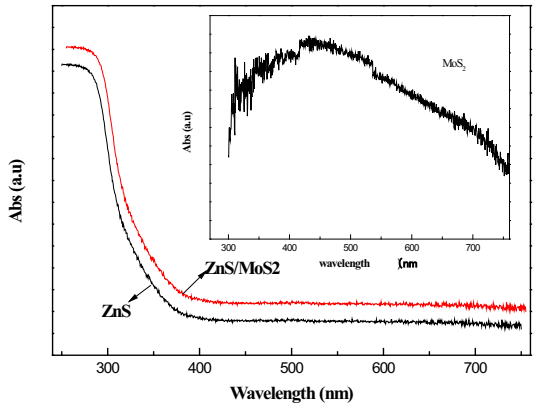

Figure 3. UV-Vis. DRS spectra of the samples ZnS, ZnS/MoS_2, the inset of Figure is UV-Vis. DRS of sample MoS_2.

The photocatalytic activities of as-prepared samples were evaluated by degrading Rhodamine B (Rh B) under UV-Vis. light irradiation. The photodegradation of the RhB as a function of the irradiation time over ZnS/MoS_2 composite is presented in Figure 4. We can see there is no significant change in the concentration curve with time when the photocatalysis is absent, which means Rh B is very stable without photocatalysis only under UV-Vis. light. From the curves of the concentration changes of RhB dye, it can be seen that the photocatalytic degradation rate of all as-prepared samples are increased with the increasing of the reaction time. In 80 minutes, nearly 70% RhB is degraded by ZnS/MoS_2. whereas in 80 minutes, the MoS_2 and ZnS degraded the RhB concentration by 64%, and 82%, respectively. It could be seen that the ZnS/MoS_2 composite exhibits the best photocatalytic activity among the samples.

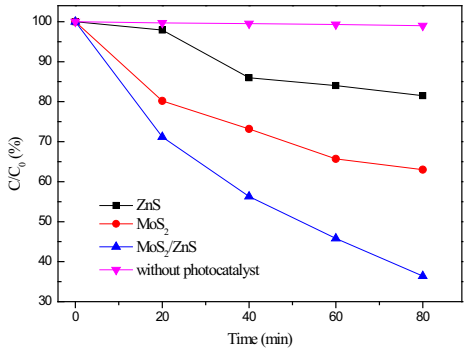

Figure 4. Photocatalytic degradation efficiency of the Rh.B over no photocatalyst, MoS_2, ZnS, ZnS/MoS_2.

In order to further confirm the enhanced conductivity of ZnS/MoS_2, CV curves of ZnS/MoS_2, ZnS, MoS_2 were measured in 0.1M phosphate buffer (pH 7.2) containing 5mM $K_3[Fe(CN)_6]$ and $K_4[Fe(CN)_6]$ as electrolyte. In Figure.5 a pair of symmertric and well-separated redox peaks was observed, indicating that the measured electroconductivity was based on the redox mechanism [14-17]. It was also noted that ZnS/MoS_2 had another cathodic peak at -700 mV may due to the redox of MoS_2. ZnS/MoS_2 exhibited higher current density than single ZnS and MoS_2 due to the accelerated electron transfer by MoS_2. This observation indicates an irreversible electrochemical reduction of MoS_2 when CV is conducted in the inorganic electrolyte at the potential range from 1000 to – 1000 mV. It means that the MoS_2 was successfully reduced.

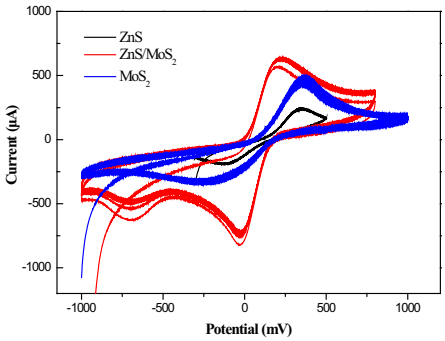

Figure 5. CV curves of MoS_2, ZnS, ZnS/MoS_2 at the scan rate of 100 mV s1 in 0.1 M PBS (pH 7.4) at RT.

It is obvious that ZnS/MoS_2 composite nanostructures possess more powerful photocatalytic capacity for the degradation of Rh B. As a consequence, a possible mechanism is proposed. According to some papers [18-21], we deduce that MoS_2 and ZnS have matching band potential.

Under irradiation, the photocatalyst could generate electrons and holes. The conduction band and valence band edge positions of MoS_2 are associated with those of ZnS, so both electrons and holes are transferred to MoS_2. Holes transfer to MoS_2 nanoflakes, which increases charge separation. Thus, MoS_2 acts as an oxidation site. In another words, the band potentials of both MoS_2 and ZnS

semiconductors are conductive to prevent the recombination of electrons and holes in the ZnS/MoS_2 composite. In general, the ZnS/MoS_2 composite with special nanostructure and interface increases the visible light absorption and restrains the recombination of electron-hole pairs.

4 Conclusion

In summary, ZnS/MoS_2 composite photocatalyst was got by two steps which in order were solvothermal methods. The microsphere of the composite was composed of hundreds of MoS_2 thin nanoplates and some ZnS plates were together with the sphere about a diameter of 1μm from the view of morphology. From the photodegradation of the Rh B organic dye we found that the ZnS/MoS_2 composited photocatalyst displayed better photocatalytic activity than both single MoS_2 and single ZnS. As a proof of concept, the ZnS/MoS_2 with good conductivity, superior electron transfer rate and high electrochemical activity is successfully used to detect photocatalytic property.

Acknowledge

This work was financially supported by a project founded by Beijing Institute of Graphic Communication (No. 27170115005/020), Project supported by Beijing Postdoctoral Research Foundation (No. 10000200272), Beijing college students' scientific research and entrepreneurial action plan (No. 22150116005/046).

References

1. Ying Wang, Mingxuan Sun, Yalin Fang, Shanfu Sun, Jia He, J. Mater. SCI, **51**, 779 2016
2. Shaohui Gao, Xuanhua Li, Jinmeng Zhu, Tengteng Tong, ingqing Wei, Small, **12**, 5692 2016
3. Shijing Liang, Zhouming Zhou, Xiuqin Wu, Shuying Zhu, Jinhong Bi, Limin Zhou, Minghua Liu, Ling Wu, Molecules, **21**. 213 2016
4. M.Nath, A. Govindaraj, C.N.R. Rao, , Adv Mater, **13**, 283, 2001
5. Lei Huang, Xiuli Wang, Jinhui Yang,Gang Liu, Jingfeng Han, Can Li, J Phys Chem C, **117** 11584 2013
6. Guoping Chen, Dongmei Li, Fan Li, Yuzun Fan, Haofei Zhao, Yanhong Luo, Richeng Yu, Qingbo Meng, Appl Catal A-Gen, **443-444**, 138 2012
7. Xiaojie Xu, Linfeng Hu, Nan Gao, Shaoxiong Liu, Swelm Wageh, Ahmed A. Al-Ghamdi, Ahmed Alshahrie, Xiaosheng Fang, Adv Functi Mater, **25**, 445 2015
8. Shengping Li, Xiuquan Gu,Yulong Zhao, Yinghuai Qiang, Shuang Zhang, Mrirong Sui, J Mater Sci-Mater EL, **27**, 386 2016
9. Lulu Long, Jiejie Chen, Xing Zhang, Aiyong Zhang, Yuxi Huang, Qing Rong, Hanqing Yu, NPG Asia Materials, **8**, doi:10.1038/am/2016.46
10. S.V Prabhakar Vattikuti, Chan Byon, Sora Jeon, Physica B, **502**, 103 2016
11. Ch. Venkate Reddy, Jaesool Shim, Migyung Cho, J Phy Chem Solids, doi.org/10.1016/j.jpcs.2016.12.011
12. Longxing Hu, Feiyan Chen, Pengfei Hu, Lianpei Zou, Xing Hua, J Mol Catal A-Chem, **411** 203 2016
13. Lu Wang, Peng Wang, Baibiao Huang, Xiaojuan Ma, Gang Wang, Ying Dai, Xiaoyang Zhang, Xiaoyan, Qin, Appl Surf Sci, **391**, 557 2017
14. Lu Han, Chengmei Liu, Shilei Dong, Caixia Du, Xiaoyong Zhang, Luhai Li, Yen Wei, Biosens Bioelectron **87**, 466 2017
15. Zhebo Chen, Dustin Cummins, Benjamin N. Reinecke, Ezra Clark, Mahendra K. Sunkare, Thomas F. Jaramill, Nano Lett, **11** 4168 2011
16. Jun Chen, Nobuhiro Kuriyama, Huatang Yuan, Hiroyuki T. Takeshita, Tetsuo Sakai, J Am Chem Soc, **123** 11813 2001
17. Shixin Wu, Zhiyuan Zeng, Qiyuan He, Zhjuan Wang, Shijie Wang, Yaping Du, Zongyou Yin, Xuping Sun, Wei Chen, Hua Zhang, Small, **8**, 2264 2012
18. Nan Tian, Zhen Li, Danyun Xu, Yang Li, Wenchao Peng, Guoliang Zhang, Fengbao Zhang, Xiabin Fan, Industrial & Engineering Chemistry Reseach, **55**, 8726 2016
19. Herme G. Baldovi, Marcos Latorre-Sancez, Ivan Esteve-Adell, Anish Khan, Abdullah M. Asiri, Samia A. Kosa, Hermenegildo Garcia, J Nanopart Res, **18**, 240 2016
20. Quanjun Xiang, Jiaguo Yu, Mietek Jaroniec, J Am Chem Soc, **134**, 6575 2012
21. Xu Zong, Hongjian Yan, Guopeng Wu, Guijun Ma, Fuyu Wen, Lu Wang, Can Li, J Am Chem Soc, **130**, 7176 2008